Cyclostationary Analysis of Electromyographic Signals

Julien Roussel, Michel Haritopoulos, Philippe Ravier, Olivier Buttelli

CYCLOSTATIONARY ANALYSIS OF ELECTROMYOGRAPHIC SIGNALS

J. Roussel, M. Haritopoulos

PRISME Laboratory
21, rue de Loigny la Bataille
28000, Chartres, France

P. Ravier, O. Buttelli

PRISME Laboratory
12, rue de Blois
45067, Orleans, France

ABSTRACT

Mean firing rate estimation is an important step in electromyographic (EMG) signals analysis. Its application is of great interest for the conception and implementation of algorithms in various research domains, ranging from neuromuscular diseases diagnosis to biomechanics. The proposed work is focused on the study of the intrinsic cyclostationary properties of single motor unit action potential train. It must be of direct interest to provide information about the neuromuscular command. It is shown that individual motor unit firing rates can be better estimated using second order cyclostationary analysis than traditional statistical tools, such as Fourier transform. After a brief state-of-the-art on cyclostationary analysis of EMG signals, the basic concepts and measures of cyclostationarity are presented. Follows a presentation of the EMG model. Results after application of the cyclostationary analysis tools for simulated and real data are provided next. A discussion on the obtained results concludes this work.

***Index Terms*—** Electromyography, Cyclostationarity, Degree of Cyclostationarity, Motor Unit, Firing Rate

1. INTRODUCTION

Neuromuscular functional unit is defined by the MU as a single functional entity [1]. This unit consists of an α-motoneuron in the spinal cord and the muscle fibers it innervates. Muscular contraction is regulated by two mechanisms: the number and the firing frequency modulation of MUs [2]. Hence, the assessment of the mean firing rate is necessary to provide information about the neuromuscular command. Some studies had referred to the cyclostationarity to investigate the neuromuscular activity without studying this property. Must of them refer to the cyclostationarity in the case of cyclic contractions [3], [4], [5], [6], [7], [8]... but, at the best of our knowledge, the cyclostationarity property has never been investigated for the electromyographic signals (EMG) in the literature.

The aim of this study is to analyse and identify the intrinsic cyclostationarity of a single motor unit (MU) action potential train (MUAPt) in the case of constant-force isometric contraction and the link with the motor units firing rate (FR). Indeed, Clamann [9] shows that under constant force and isometric condition, the inter-spike intervals (ISI) are not constant but random (jitter). It makes the signal non-periodic and thus, the spectrum density does not contain any relevant information about the firing rates. We show in this work that a cyclostationnary analysis can reveal this mean firing rates.

Knowing the mean firing rates is of importance for designing MU-decomposition and/or MU-source separation methods. Final applications of this work can be found in neuromuscular diseases diagnosis or in biomechanics studies.

2. CYCLOSTATIONARY ANALYSIS

A cyclostationary (CS) signal is referred to a time-variant process with periodic statistical properties [10]. More specifically, a wide-sense first order CS signal shows a periodic instantaneous mean: $m_x(t) = m_x(t+T)$, while a second order CS (periodically correlated process) shows a periodic auto-correlation function: $\Gamma_{xx}(t,\tau) = \Gamma_{xx}(t+T,\tau)$, where $\Gamma_{xx}(t,\tau)$ stands for the auto-correlation function of x at time-location t and time-lag τ. The two-dimensional Fourier transform along t and τ of the auto-correlation function provides the cyclic spectral density (CSD) $S_{xx}(f,\alpha)$:

$$S_{xx}(f,\alpha) = \iint_{t,\tau\in\mathbb{R}} \Gamma_{xx}(t,\tau)\, e^{-2i\pi(f\tau+\alpha t)} dt d\tau \qquad (1)$$

with $\alpha = \frac{n}{T}\ \forall n \in \mathbb{N}$. The CSD can be efficiently estimated using the averaged cyclic periodogram technique [11]. The CSD of eq.1 can be rewritten as a spectral correlation between $X\left(f+\frac{\alpha}{2}\right)$ and $X\left(f-\frac{\alpha}{2}\right)$ [12]:

$$S_{xx}(f,\alpha) = \mathbb{E}\left[X\left(f-\frac{\alpha}{2}\right)\overline{X\left(f+\frac{\alpha}{2}\right)}\right] \qquad (2)$$

In this work, we are interested in highlighting the presence of cyclostationary components in EMG data. Basically, this can be done by analysing the CSD distribution that is theoretically non zero whenever $\alpha \neq 0$. We are also interested in estimating cyclic frequencies values that may be present in the data. So we focus on marginal distributions of CSD as a function of the cyclic frequency α.

A first measure of cyclostationarity is the integrated CSD over spectral frequency f. Randall *et al.* [13] showed that this measure can be easily computed using the expectation value of the Fourier transform of the squared magnitude of $x_h(t)$, with $x_h(t)$ being the Hilbert transform of $x(t)$:

$$M_{xx}(\alpha) = \int S_{xx}(f,\alpha)\, df \equiv \mathbb{E}\left[FT[|x_h(t)|^2]\right] \quad (3)$$

The Hilbert transform magnitude is often used to extract the envelope of any signal so that this computation procedure of $M_{xx}(\alpha)$ will be referred to envelope analysis in the following of the paper.

Another measure of cyclostationarity is the power- normalised version of the integrated CSD, also named cyclostationary degree [14]:

$$DCS_{xx}(\alpha) = \frac{M_{xx}(\alpha)}{M_{xx}(0)} \quad (4)$$

3. MODELISATION

Each MUAPt $y_i(t)$ is simulated using a spike train convolved with the MUAP template, namely $x_i(t)$, where i stands for the MUAP index ($i \in [1; N]$, with N the number of active MUs). In [9], ISI is defined as a Gaussian process with mean firing period $T_i = FR_i^{-1}$ and standard deviation s_i computed using the following relation for the *biceps brachii*:

$$s_i = 0.91 \cdot FR_i^{-2} + 4 \cdot 10^{-3} \quad (5)$$

expressed in seconds. Hence, the MUAPt $y_i(t)$ is modeled as follows:

$$y_i(t) = x_i(t) * \sum_{n=-\infty}^{+\infty} \delta(t - nT_i + \tau_i) \quad (6)$$

with $\tau_i \sim \mathcal{N}(0, s_i^2)$. Finally, the full EMG signal writes as a sum of all active MU contributions:

$$EMG(t) = \sum_{i=1}^{N} y_i(t) + n(t) \quad (7)$$

where $n(t)$ is an i.i.d. Gaussian noise with σ_n^2 its variance.

In [13], the authors give the expression of the cyclic spectrum density in a more complicated model than our model (eq.6) and its adaptation results, i.e. without amplitude modulation, in the following expression:

$$\begin{aligned} S_{y_iy_i}(f,\alpha) = \;& \tfrac{1}{T} S_{x_ix_i}(f,\alpha)\left[\Phi_i(\alpha) - S_{\Phi_i\Phi_i}(f,\alpha)\right] \\ & \times \textstyle\sum_{k\in\mathbb{Z}} \delta(\alpha - \frac{k}{T_i}) \end{aligned} \quad (8)$$

where $S_{\Phi_i\Phi_i}(f,\alpha) = \Phi_i(f+\frac{\alpha}{2})\overline{\Phi_i(f-\frac{\alpha}{2})}$, $S_{x_ix_i}(f,\alpha) = X_i(f+\frac{\alpha}{2})\overline{X_i(f-\frac{\alpha}{2})}$ with $X_i(f) = FT[x_i(t)]$, $\Phi_i(f)$ being the Fourier transform of the probability density of τ_i and $S_{nn}(f)$ being the spectrum density of noise. The case $\alpha = 0$ gives us the spectrum density of y_i:

$$S_{y_iy_i}(f,0) = \frac{1}{T_i} S_{x_ix_i}(f,0)\left[1 - |\Phi_i(f)|^2\right] \quad (9)$$

According to the authors, $\Phi_i(f)$ is a low-pass filter where cut-off frequency at $-3dB$ is approximately equal to $f_0 = \frac{0.187}{s_i}$ and using eq.5 we get $f_0 = \frac{1}{4.86\times FR_i^{-2}+21.3\times 10^{-3}}$. For a firing rate varying between $5Hz$ and $25Hz$ we obtain a $-3dB$ cut-off frequency between $4.64Hz$ and $34.35Hz$.

It can be deduced that $S_{y_iy_i}(f,0) \approx \frac{1}{T}S_{x_ix_i}(f,0)$ because the spectrum density of MUAP waveform $S_{x_ix_i}(f,0)$ is negligible for all $f < 25Hz$. This assumption can be extended to the CSD case, so we have $S_{\Phi_i\Phi_i}(f,\alpha)S_{x_ix_i}(f,\alpha) \approx 0$ and using eq.3 the envelop analysis of y_i can be written as follows:

$$M_{y_iy_i}(\alpha) = \frac{1}{T}\left(\sum_{k\in\mathbb{Z}} \delta(\alpha - \frac{k}{T_i})\right)\Phi_i(\alpha) M_{x_ix_i}(\alpha) \quad (10)$$

4. SIMULATION STUDY

4.1. Simulation Model

Synthetic EMG signals are generated using an EMG MUAP library template. Fig.1 shows a time plot of this signal. From now on, in order to clearly identify their contributions, let $N = 3$ be their number with firing rates, expressed in Hz: $FR_i = [10, 12, 15]\, \forall i \in \{1, 2, 3\}$.

Signals are computed using various jitter levels as a rate of the Clamann's law (eq.5): $10\% s_i$, $50\% s_i$ and $100\% s_i$ without noise; $100\% s_i$ with 10dB noise..

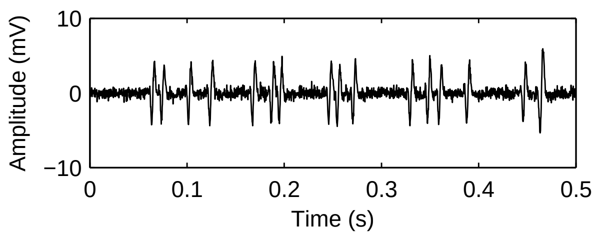

Fig. 1. Representation of the simulated EMG signal with three active MUAPs and $10dB$ Gaussian noise added.

4.2. Envelope Analysis

The envelope analysis $M_{xx}(\alpha)$ of the previously simulated MUAPt using eq.7, is computed without noise and with a $10dB$ additive noise. Fig.2 and Fig.3 show plots of the Fourier transform and the Fourier transform of the envelop, respectively. We limit the frequency axis to $40Hz$ in order to view the mean firing frequencies and their first harmonics.

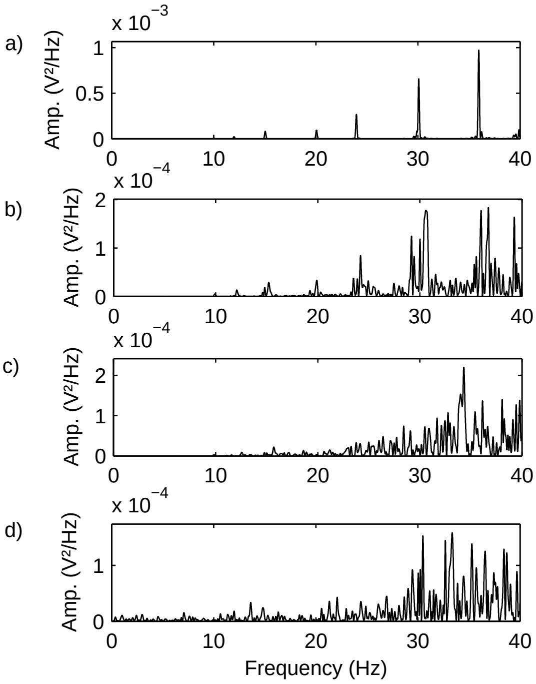

Fig. 2. Fourier transform of the simulated signal with a) 10% b) 50% c) 100% of Clamann's law in the unnoisy case and d) 100% of Clamann's law with $10\ dB$ Gaussian noise added.

In the noiseless case, Fourier transform of Fig.2(a-c) exhibits only a small peak at $15Hz$ corresponding to the firing frequency of the third MU, but with a $10dB$ noisy signal all significant peaks in the Fourier transform are buried in noise as shown in Fig.2d. We observe that EMG spectra are energetical for frequencies above 20 Hz. This is verified for all the graphs in Fig.2a-d. As a consequence, the harmonics are found to be predominant for low percentage values of the Clamann's law (2a).Increasing the σ_i values will make the periodicity disappear and the harmonics vanish. On the contrary, the envelop analysis, in Fig.3, improves the low frequency identification and one can easily identify on noiseless figures the contributions of the three motor units. This is essentially due to the low pass filter effect of the jitter functions (eq.10) annihilating the high frequency parts of the spectrum. From Fig.3a to c, the increasing of jitter rates decreases the harmonic firing rates. This is due to the $-3dB$ cut-off frequencies of the filter, $\Phi_i(\alpha)$ in eq.10, that decrease from 230 Hz to 46 Hz and 23 Hz in the case of 10%, 50% and 100% of

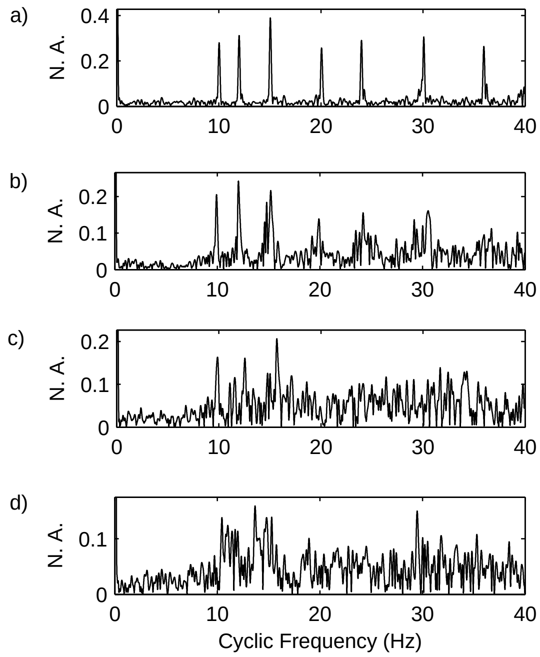

Fig. 3. DCS of the same signal with a) 10% b) 50% c) 100% of Clamann's law in the unnoisy case and d) 100% of Clamann's law with $10\ dB$ Gaussian noise added - Normalised Amplitude (N.A.) y-axis.

Clamann's law, respectively (cut-off frequency values corresponding to the highest 15 Hz MUAPt frequency). This also explains the decreasing of power by 1.4 concerning the fundamental frequencies.

5. REAL EMG STUDY

5.1. EMG Signals and protocols

Real intramuscular EMG (iEMG) signals were provided by EMGLab [15]. One signal is selected with constant percentage of maximum voluntary contraction $10\%MVC$ and under isometric condition, recorded using bipolar fine-wire electrodes on the right *biceps brachii* muscle. A dynamo-meter was used to control the muscle force that ensured a low ripple during $10s$ of measurement. A $15s$ rest before each measurement and a two minutes break between two different force levels are realised in order to avoid muscle fatigue effects.

5.2. Decomposition Statistical Analysis

Intramuscular EMG signals can be decomposed using pattern matching methods in order to retrieve their single motor units components. The R00701 signal was manually decomposed using the EMGLab(V1.03) software [16] and firing patterns were statistically analyzed in order to assess the mean firing rate and jitter standard deviation. Figure 4 shows the first hundred milliseconds of the EMG signal, with its MUAP markers.

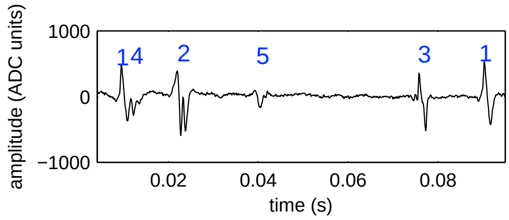

Fig. 4. Representation of the real iEMG signal named R00701 (10%MVC).

The decomposition of the R00701 signal reveals five active motor units, identified by their number on Fig.4. Table 1 shows, for each detected MU (corresponding number reported in column 1), the mean ISI value, the standard deviation of the ISI sequence and the mean firing rate in column two, three and four respectively. A minimum of hundred realizations for each MU ensured a correct estimation of both mean and standard deviation values.

MU	$T_{fr}(ms)$	$\sigma_{T_{fr}}(ms)$	$F_{fr}(Hz)$
1	89.25	8.30	11.30
2	93.25	8.28	10.81
3	85.24	9.36	11.87
4	91.91	8.33	10.97
5	75.42	6.48	13.36

Table 1. Statistical analysis of R00701 signal.

The mean firing rates were computed using the inverse ISI values: $F_{fr} = \frac{1}{M}\sum_{j=1}^{M}\frac{1}{ISI_j}$ where M is the number of MUAP occurrences.

5.3. Envelope Analysis

The Fourier transform and the DCS (eq.4), are computed and plotted on Fig.5 and Fig.6 respectively.

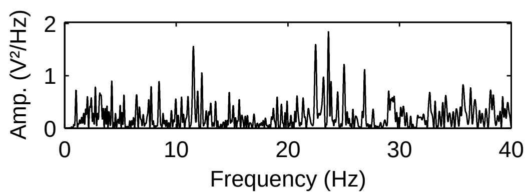

Fig. 5. Fourier transform of the R00701 iEMG signal.

Similarly to the analysis in the simulation case, the firing frequency peaks are buried in noise in the Fourier transform (Fig.5) and does not reveal the firing rates.

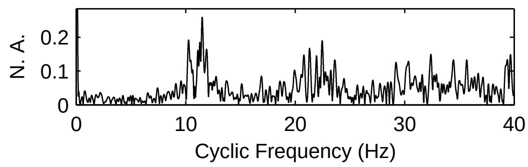

Fig. 6. Degree of cyclostationarity of the R00701 iEMG signal.

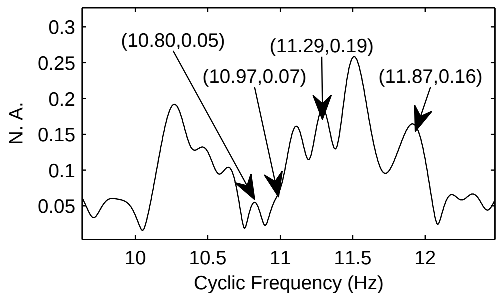

Fig. 7. DCS of the R00701 iEMG signal - Zoom. The mean FR values of table 1 are reported on the graph.

Fig.6 contains spectral lines with a first amount of data concentrated around the frequency range from $10Hz$ to $12.5Hz$. The mean firing frequency values reported in table 1 are contained within the same frequency range excepted for the last MU located at $13.36Hz$. A second amount of data from $20Hz$ to $26Hz$ corresponds to the first harmonics range, and finally, a third one corresponds to the second harmonics range. It can be observed that, contrary to the first frequency range from $10Hz$ to $12.5Hz$, spectral lines are clearly spread over their first and second harmonics frequency range. Fig.7 is a zoom of Fig.6 around frequency range $[10, 12.5]$ Hz and the expected frequency values are represented with labeled arrows. One observes in Fig.4 that MUAPs 4 and 5 have lower amplitude than the others and that explains the difficulty to find these harmonics in the DCS.

6. DISCUSSION

In [17] it is shown that the power spectrum of the rectified signal, which is an approximation of the envelop, enhances the low-frequency peaks, but there is no theoretical justifications on this. Using the single spike train model of eq.6, the authors of [13] show that the signal is not periodic, but second-order periodic due to the jitter. That means the power spectrum density (eq. 9) does not reveal any periodicity hence the need of a second order anlaysis tool such as CSD or envelop analysis.

They show that the CSD (eq.8) gives a line spectrum along cyclic frequencies at the mean MU firing rates and, hence, it becomes a useful tool in order to reveal the second order periodicities. Finally, they prove that the envelop analysis is equal to the integration of the CSD along the spectrum frequencies; hence, ideally, the envelop analysis exhibits a spectrum line at the mean firing rates. In this work [13], it has been also theoretically proven, in eq.10, that the random jitter acts only as a low-pass filter in the envelop analysis.

In practice, probably due to the highly stochastic nature of data, one observes a degradation of the line spectrum and thus, a lack of precision of the estimated mean firing rate, as one can see in Fig.3 and Fig.7. Furthermore, since the jitter acts as a set of low-pass filters which cut-off frequencies fall in the same frequencies as the mean firing rates, the harmonic magnitudes are strongly attenuated. Jitter has a low-pass frequency approximately equal to the mean firing rates which strongly decreases the harmonics magnitude.

These limitations prevent a correct analysis of a high number of active MUs. At the time being, the method is effective for analyzing a small number of active MUs, i.e., for low MVC level (about $10\%MVC$ in the case of bipolar iEMG signals). Implementation of a more advanced approach is necessary to identify MUs activity in a higher level of contraction.

As a conclusion, we showed in this paper that we were able to retrieve individual firing rates, firstly, theoretically, by an envelope analysis based on an appropriate model of MUAPt; secondly, by estimating the envelope on synthetic data, when a small number of active MUs is considered; thirdly, experimentally, by identifying FR values that were previously measured on temporal data.

7. REFERENCES

[1] J. C. Eccles and Charles S. Sherrington, "Numbers and contraction-values of individual motor-units examined in some muscles of the limb," *Proceedings of the Royal Society of London. Series B, Containing Papers of a Biological Character*, vol. 106, no. 745, pp. 326–357, 1930.

[2] John V. Basmajian and Carlo J. De Luca, *Muscles alive, their functions revealed by electromyography*, Williams & Wilkins, 1967.

[3] G Balestra, S Frassinelli, M Knaflitz, and F Molinari, "Time-frequency analysis of surface myoelectric signals during athletic movement," *Engineering in Medicine and Biology Magazine*, vol. 20, no. 6, pp. 106–15, 2001.

[4] P Bonato, S H Roy, M Knaflitz, and C J De Luca, "Time-frequency parameters of the surface myoelectric signal for assessing muscle fatigue during cyclic dynamic contractions," *Biomedical Engineering, IEEE Transactions on*, vol. 48, no. 7, pp. 745–53, July 2001.

[5] Hua Cao, Imad El Hajj Dib, Jérôme Antoni, and Catherine Marque, "Analysis of muscular fatigue during cyclic dynamic movement," *EMBS Engineering in Medicine and Biology Society*, vol. 2007, pp. 1880–3, Jan. 2007.

[6] M. Knaflitz and Paolo Bonato, "Time-frequency methods applied to muscle fatigue assessment during dynamic contractions," *Journal of Electromyography and Kinesiology*, vol. 9, no. 5, pp. 337–50, Oct. 1999.

[7] J.S. Karlsson, N. Östlund, B. Larsson, and B. Gerdle, "An estimation of the influence of force decrease on the mean power spectral frequency shift of the emg during repetitive maximum dynamic knee extensions," *Journal of Electromyography and Kinesiology*, vol. 13, no. 5, pp. 461–468, Oct. 2003.

[8] E Serpedin, F Panduru, I Sari, and Georgios B. Giannakis, "Bibliography on cyclostationarity," *Signal Processing*, vol. 85, no. 12, pp. 2233–2303, Dec. 2005.

[9] H. Peter Clamann, "Statistical analysis of motor unit firing patterns in a human skeletal muscle," *Biophysical journal*, vol. 9, no. 10, pp. 1233–51, Oct. 1969.

[10] W. R. Bennett, "Statistics of regenerative digital transmission," *The Bell System Technical Journal*, vol. 1, pp. 1501–1542, 1958.

[11] Roger Boustany and Jérôme Antoni, "Cyclic spectral analysis from the averaged cyclic periodogram," in *Proceedings of the 16th IFAC World Congress Prague Czech Republic*, 2005.

[12] William A. Gardner, "The spectral correlation theory of cyclostationary time-series," *Signal processing*, vol. 11, pp. 13–36, 1986.

[13] Robert B. Randall, Jérôme Antoni, and S. Chobsaard, "The relationship between spectral correlation and envelope analysis in the diagnostics of bearing faults and other cyclostationnary machine signals," *Mechanical Systems and Signal Processing*, vol. 15, no. 5, pp. 945–962, 2001.

[14] Goran D Živanović and William A Gardner, "Degrees of cyclostationarity and their application to signal detection and estimation," *Signal Processing*, vol. 22, no. 3, pp. 287–297, Mar. 1991.

[15] P. A. Mathieu, "[online dataset r007, available at http://www.emglab.net]," .

[16] K. C. McGill, Z. C. Lateva, and H. R. Marateb, "Emglab: an interactive emg decomposition program," *J Neurosci Methods*, vol. 149(2), pp. 121–133, 2005.

[17] Dario Farina, Roberto Merletti, and Roger M. Enoka, "The extraction of neural strategies from the surface emg.," *Journal of Applied Physiology*, vol. 96, no. 4, pp. 1486–95, Apr. 2004.